MONOLITHIC COMPLIANT MECHANISM FOR AN EMFC MASS COMPARATOR WEIGHING CELL

M. Darnieder[1], M. Wittke[1], M. Pabst[2], T. Fröhlich[2], R. Theska[1]

Technische Universität Ilmenau, Department of Mechanical Engineering
[1] Institute for Design and Precision Engineering, Precision Engineering Group
[2] Institute of Process Measurement and Sensor Technology, Process Measurement Group

ABSTRACT

Mass comparator weighing cells based on electromagnetic force compensation (EMFC) find application in the most demanding force and mass measurement applications. The centerpiece of these devices is a highly sensitive compliant mechanism with thin flexure hinges. The compliant mechanism forms the mechanical part of the mechatronic overall system. A novel mechanism based on an advanced adjustment concept has been developed, manufactured, and experimentally investigated. The adjustment is designed to further reduce the measurement uncertainty for mass comparisons by canceling out first-order error c omponents. The focus is on the mechanical properties: stiffness, tilt sensitivity, and off-center load sensitivity. The elastic stiffness of the compliant mechanism is compensated by introducing a negative gravitational stiffness to enable the compensation of manufacturing deviations and to increase mass resolution.

Index Terms - electromagnetic force compensation, mass comparator, adjustment, elastic stiffness, gravitational stiffness, finite element model, semi-circular flexure hinge

1. INTRODUCTION

Prototype mass comparators are used to determine minute mass differences between masses of virtually the same nominal mass, e.g. the comparison of two 1 kg reference standards. The new definition of the unit kilogram based on the PLANCK constant pave the way for in vacuo comparison of reference masses and thus a further reduction of the measurement uncertainty. Here, mechanical error sources stemming from a the stiffness of the mechanism, its tilt sensitivity, and the off-center load sensitivity are limiting the achievable metrological performance of mass comparators. The development of the presented weighing cell concept aims at an elimination of first-order error components by design and adjustment.

Commercially available mass comparators are carefully balanced electromagnetic force compensation (EMFC) weighing cells. The weighing cells consist of a mostly monolithic mechanism with flexure h inges, a fi xed co unter ma ss an d an el ectromagnetic fo rce compensation (EMFC). To minimize the elastic stiffness, the flexure hinges have a minimum notch height or minimum thickness of 50 μm. The schematic of the mechatronic system is presented in Figure 1. The mechanism of the weighing cell consists of a parallelogram linkage which is guiding the weighing pan (A-B-C-D). The counter force acting on the weighing pan is generated by the transmission lever system (F-G-H) and a counter mass (L). The EMFC system allows for accurate position control of the mechanism. It includes a position sensor (M) and a voice coil actuator (K). The current through the voice coils is a measure for the force imbalance of the

mechanism. By calibration, this value can be associated with a mass. A mass comparator is designed for a small weighing range around the nominal mass. Two masses are compared by substitution weighing - the masses are subsequently placed on the weighing pan.
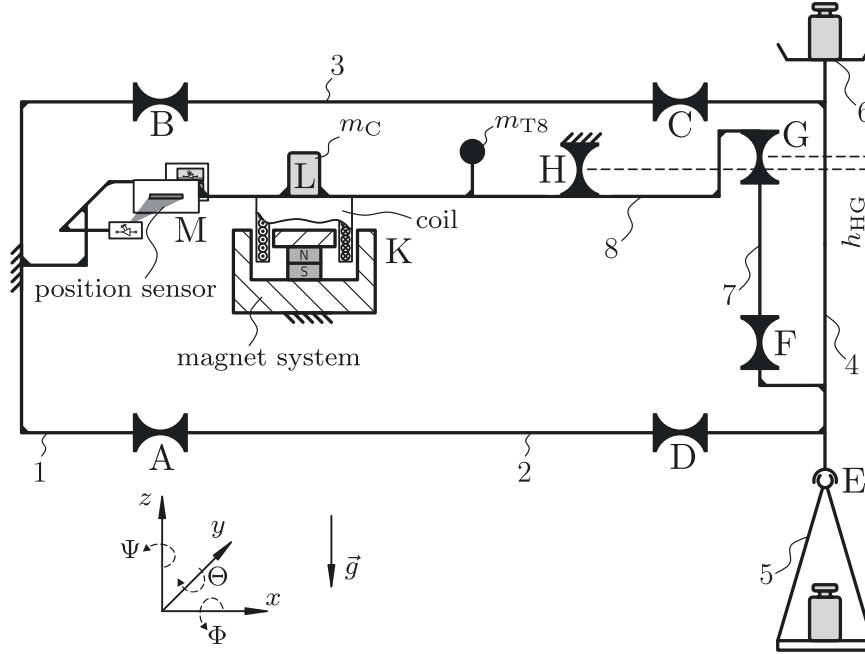

Figure 1: Schematic of an electromagnetic force compensated weighing cell after [1] Depicted adjustment measures are the trim mass m_{T8} and the vertical distance between pivot H and G (h_{HG}).

Mechanical imperfections of the weighing cell mechanism make the system susceptible to changing environmental conditions. These mechanical first-order error components need to be reduced to small residual values. From previous experiments, two main challenges for canceling out mechanical fist-order error components are known: cross-sensitivities between the mechanical parameters and the compensation of manufacturing deviations.
Cross-sensitivities especially related to off-center loads and tilt angles are mutually affecting the adjustment state in terms of tilt sensitivity and off-center load sensitivity. The weighing cell design needs to be optimized to reduce the mentioned cross-sensitivities.
Manufacturing deviations at the flexure hinges and the correlated scattering of the elastic stiffness represent a major challenge. Fine adjustment of the stiffness is thus indispensable. The present paper describes the development of the weighing device from concept to the first experimental tests and measurements.

2. CONCEPT DEVELOPMENT

The vertical distance between the flexures H and G in the weighing cell introduce a gravitational stiffness component that is typically referred to as astatization. The linearized equation for the gravitational stiffness effect reads: $-h_{HG}\, m_G\, g$. Either the vertical distance h_{HG} or the gravitational force of m_G can be varied to manipulate the astatization effect. The manipulation of h_{HG} is not pursued due to anticipated downsides of potential design solutions. The second option,

the variation of the gravitational force, is known as substitution. Substitution on the weighing pan strongly affects the electrical zero of the weighing cell. Branching the force flow through two independent lever systems enables the introduction of two or more h_{HG}-values. The stiffness can thus be adjusted maintaining a constant electrical zero by altering the force balance between the load paths. The key aspect of the novel adjustment concept is the branching of the force flow through multiple lever systems, see Figure 2.
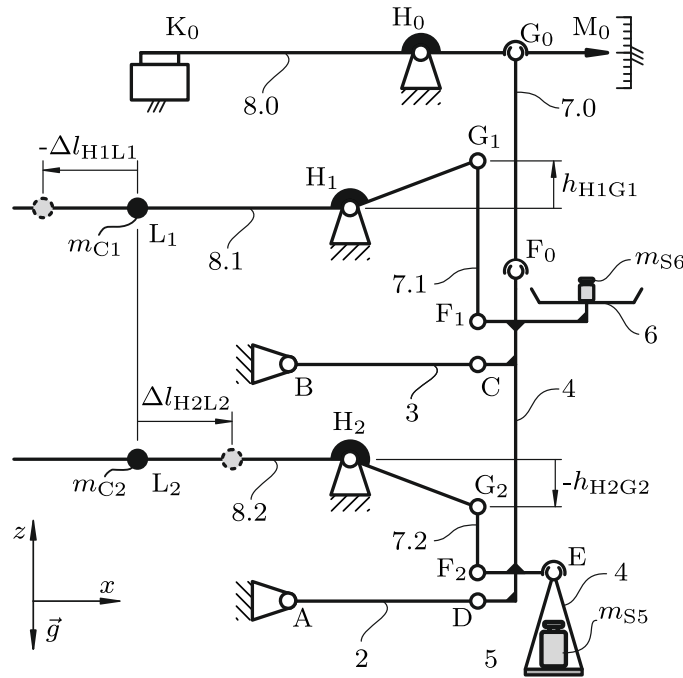

Figure 2: Concept of the novel weighing system with model parameters and an exemplary setting of h_{H1G1} and h_{H2G2}. The joints at G_0, F_0, and E represent two-axis flexure hinges with two degrees of freedom.

The concept for the weighing cell design was fundamentally based on the *separation of functions* principle, ensuring that each functional unit can be optimized for its specific function. In precision measurement devices the separation into a force- and a metrology loop is highly beneficial (e.g. [2]).

In a mass comparator, the force- and the metrology loop are inherently coupled and cannot be fully separated. However, the main force flow can be divided into a high- and low-force subsystem, of which the latter is the measurement system (metrology loop). This concept takes advantage of the small electrical weighing window of a 1 kg-mass comparator: ± 2 g. It was realized by a third lever (8.0) in Figure 2. The small force differences to the nominal mass are guided through the third lever (8.0), which holds the EMFC system. The so called *measurement lever* is characterized by $h_{H0G0} = 0$ mm and its center of gravity is located at the center of rotation of its main flexure H_0.

As indicated in Figure 2, the flexure hinges F_0 and G_0 are two-axis flexure hinges to weaken the y constraint between the high- and low-force system. As a result, unavoidable deformations of the force transmission system in y direction show only minor effects on the measurement lever. The reduced lateral deflections within the EMFC components mitigate the cross-sensitivities of the mechanical properties which is the effect of ground tilt on the off-center load sensitivity and

the effect of an off-center load on the tilt sensitivity.

The kinematic structure is depicted in Figure 2. The levers 8.1 and 8.2 provide the stiffness adjustment capability whereas the measurement lever 8.0 mitigates the cross-sensitivities of the weighing cell. Horizontally relocatable counter masses on levers 8.1 and 8.2 enable the manipulation of the force balance between the levers without changing the static equilibrium of the overall system. The mechanical stiffness of the mechanism is adjustable. Assuming equal masses and displacements, this was achieved by shifting both counter masses alongside the levers - in opposing direction.

The rotational stiffness variation of the two-lever mechanism is described as:

$$\Delta C_{\text{rot,grav}} = \left(\frac{h_{\text{H1G1}}^2}{h_{\text{F1G1}}} - h_{\text{H1G1}} \right) \Delta F_{\text{G1}} + \left(\frac{h_{\text{H2G2}}^2}{h_{\text{F2G2}}} - h_{\text{H2G2}} \right) \Delta F_{\text{G2}} \tag{1}$$

The stiffness variation is defined for each lever by the force at G_i, and the parameters h_{HG} and h_{FG}. The change of the forces through G_1 and G_2 is key to the function principle and is described as a horizontal displacement of the counter mass on the respective lever:

$$\Delta F_{\text{Gi}} = -m_{\text{Ci}}\, g\, \Delta l_{\text{HiLi}} \frac{1}{l_{\text{HG}}} \tag{2}$$

Combining Eqs. (1) and (2) yields:

$$\Delta C_{\text{rot,grav}} =$$
$$\left(-\left(\frac{h_{\text{H1G1}}^2}{h_{\text{F1G1}}} - h_{\text{H1G1}} \right) m_{\text{C1}}\, \Delta l_{\text{H1L1}} - \left(\frac{h_{\text{H2G2}}^2}{h_{\text{F2G2}}} - h_{\text{H2G2}} \right) m_{\text{C2}}\, \Delta l_{\text{H2L2}} \right) \frac{g}{l_{\text{HG}}}$$

Assuming equal masses and contrary displacements on levers 8.1 and 8.2 ($\Delta l_{\text{HL}} = \Delta l_{\text{H1L1}} = -\Delta l_{\text{H2L2}}$), the equation for the stiffness change with ($m_{\text{C}} = m_{\text{C1}} + m_{\text{C2}}$, $h_{\text{H1G1}} > h_{\text{H2G2}}$, $h_{\text{F1G1}} > 0$, $h_{\text{F2G2}} > 0$) reads:

$$\Delta C_{\text{rot,grav}} = \frac{1}{2} \left(-\left(\frac{h_{\text{H1G1}}^2}{h_{\text{F1G1}}} - h_{\text{H1G1}} \right) + \left(\frac{h_{\text{H2G2}}^2}{h_{\text{F2G2}}} - h_{\text{H2G2}} \right) \right) m_{\text{C}}\, \Delta l_{\text{HL}} \frac{g}{l_{\text{HG}}}$$

The stiffness variation at the weighing pan is described as:

$$\Delta C_{\text{grav}} = \frac{1}{2}\, m_{\text{C}}\, \Gamma\, \Delta l_{\text{HL}} \frac{g}{l_{\text{HG}}^3} \tag{3}$$
$$\text{with } \Gamma = (h_{\text{H1G1}} - h_{\text{H2G2}}) + \frac{h_{\text{H2G2}}^2 h_{\text{F1G1}} - h_{\text{H1G1}}^2 h_{\text{F2G2}}}{h_{\text{F1G1}}\, h_{\text{F2G2}}}.$$

The stiffness of the weighing system can thus be adjusted before and even during operation according to (3).

3. MONOLITHIC WEIGHING CELL DESIGN

The novel weighing cell structure has three main functional subsystems. These are:

- quasi-linear guide $(2, 3, 4)$

- force transmission system $(7.1, 7.2, 8.1, 8.2)$
- measurement system $(7.0, 8.0)$

Their arrangement within the monolithic weighing cell is critical to performance, machinability, and mountability. Many designs for EMFC weighing cells feature the force transmission within the parallelogram linkage of the linear guide. This arrangement generally leads to a larger parallelogram linkage which decreases both stiffness and off-center load sensitivity in the *x* direction. For the current weighing cell design, manufacturing and mounting accessibility demanded the lever systems (force transmission system, measurement lever) outside of the parallelogram guide. The levers were stacked on top of the parallelogram guide.
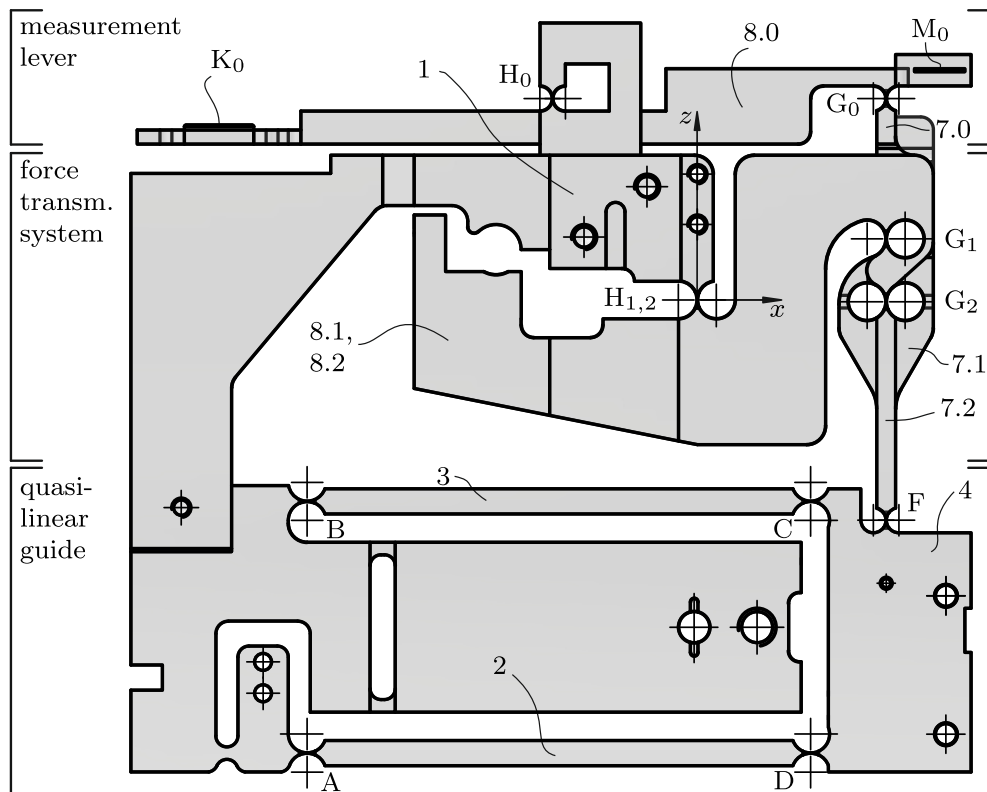

Figure 3: Monolithic setup of the weighing cell prototype separated into three functional groups: linear guide $(2, 3, 4)$, force transmission $(7.1, 7.2, 8.1, 8.2)$, measurement lever $(7.0, 8.0, K_0, M_0)$.

The force transmission system, see central area in Figure 3, which was designed as a two-lever system, needed to be realized without negatively affecting other properties of the weighing cell mechanism. To this end, especially the arrangement of the levers and their respective coupling elements is crucial. The intended change in force distribution from one lever (8.1) to the other (8.2) introduces a systematic off-center load on the load carrier (4) if the coupling elements were attached at different lateral positions. The choice fell on a design with nested levers and symmetry in the *y* direction to circumvent the mentioned introduction of off-center loads and to achieve a compact design. The arrangement is optimized in terms of function at cost of a more complex manufacturing process.

An overview of the nested lever system excluding the parallelogram guide and base is provided in Figure 4. The main difference between the central lever (1) and the outer lever (2) is the

different value for h_{HG} which can be visually identified in Figure 4. The central lever (1) is equipped with the larger positive h_{H1G1} value whereas the outer lever (2) even has a slightly negative h_{H2G2} value. Increasing the force flow through the central lever (1) and reducing the force flow through the outer lever (2) thus leads to a decrease in stiffness and vice versa.
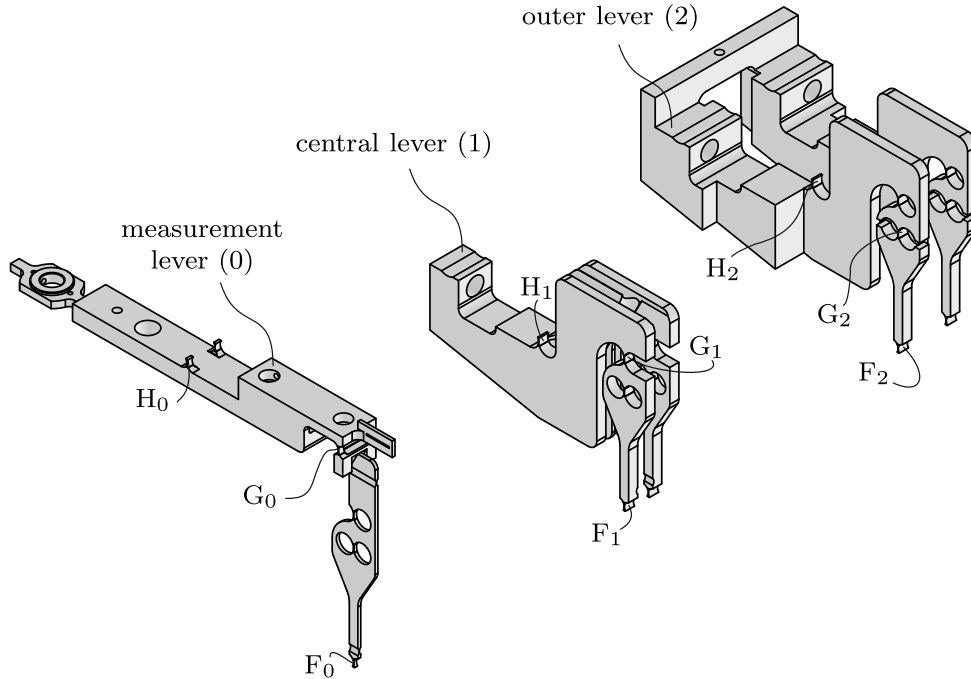

Figure 4: Exploded view of the nested lever system.

The measurement lever was located on top of the weighing cell. The measurement lever implements a stable metrology loop within the mass comparator weighing cell. The lever directly interfaces with the EMFC components. Its lateral error motions should therefore be minimized. The maximum force flow through the lever was limited to an equivalent of $\pm 2\,\mathrm{g}$ - the electrical weighing range of the prototype mass comparator. A direct consequence is the absence of a rather heavy counter-mass that tends to deflect the lever laterally for $\Phi \neq 0$. Contrarily, by design and adjustment, its center of mass can be directly positioned to the center of rotation (CoR), which minimizes any tilt-induced deformations.

The aperture slit was located directly above the coupling element. The lever is suspended by two flexure hinges in the middle, in proximity to the base connection of the weighing cell. The coil and the magnet system were mounted on the opposite side of the equal-arm measurement lever.

The measurement lever's coupling element was placed inside the nested coupling elements of the force transmission system with additional compliance in the y direction. The length of the coupling element was maximized to minimize the undesired mechanical coupling between the force transmission- and the measurement system in the x and y direction. The pivots F_0 and G_0 were designed as two-axis flexure hinges. For a simpler manufacturing, their perpendicular axes have an offset in the z direction. The laterally compliant mechanical coupling of the subsystems minimizes the transfer of lateral deflections to the measurement lever. These lateral deflections of the force transmission system result from ground tilt or off-center loads on the weighing pan. All sources of heat dissipation within the EMFC system, the coil, and the po-

sition sensor's optoelectronic components, were placed on top of the mechanism to minimize thermal influences.

3.1. STIFFNESS ADJUSTMENT

The weighing system was designed to allow both stiffness and tilt sensitivity to be adjusted independently through the displacement of trim masses. The elastic stiffness of the mechanism in Fig. 2 is described with (4):

$$
\begin{aligned}
C_{\text{el}} = {} & (C_A + C_B + C_C + C_D) \cdot l_{\text{AD}}^{-2} \\
& + \left(C_{\text{F0}} \left(\frac{h_{\text{H0G0}}}{h_{\text{F0G0}}} \right)^2 + C_{\text{G0}} \left(1 - \frac{h_{\text{H0G0}}}{h_{\text{F0G0}}} \right)^2 + C_{\text{H0}} \right) l_{\text{H0G0}}^{-2} \\
& + \left(C_{\text{F1}} \left(\frac{h_{\text{H1G1}}}{h_{\text{F1G1}}} \right)^2 + C_{\text{G1}} \left(1 - \frac{h_{\text{H1G1}}}{h_{\text{F1G1}}} \right)^2 + C_{\text{H1}} \right) l_{\text{H1G1}}^{-2} \\
& + \left(C_{\text{F2}} \left(\frac{h_{\text{H2G2}}}{h_{\text{F2G2}}} \right)^2 + C_{\text{G2}} \left(1 - \frac{h_{\text{H2G2}}}{h_{\text{F2G2}}} \right)^2 + C_{\text{H2}} \right) l_{\text{H2G2}}^{-2}
\end{aligned} \tag{4}
$$

The required adjustment range for the coarse adjustment has been designed based on the uncertain input parameters defined by the manufacturing tolerances for the monolithic mechanism. The most decisive parameter, the minimal notch height of the flexure hinges h, was assigned with the tolerance $\pm 5\,\mu\text{m}$. The results of the MONTE CARLO calculation for the adjustment parameters l_{H1L1} and l_{H2L2} are presented as probability density function in Fig. 5. Due to retrospective design changes to the mechanism, the calculated mean position for each counter mass is slightly eccentric to the adjustment range. All considered input parameter deviations can be
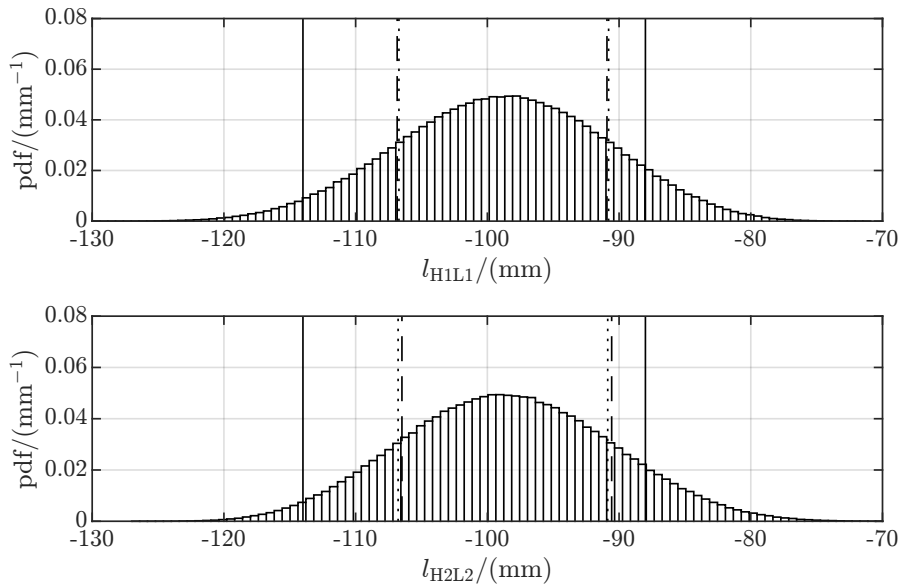

Figure 5: Probability distribution of the calculated positions for the counter weights on lever 8.1 and 8.2 to achieve a static equilibrium and zero stiffness. The solid vertical lines restrict the actual adjustment range of the realized prototype.
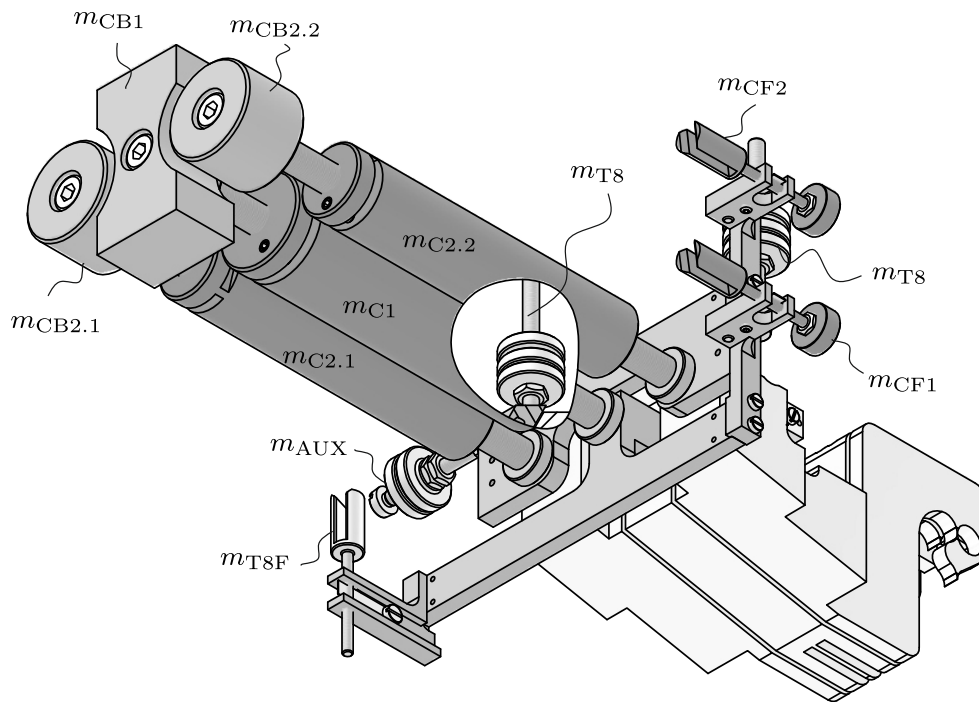
Figure 6: Designation of the masses attached to the free end of the force transmission lever system.

compensated with a probability larger than $68\,\%$.

The trim masses on the force transmission system are depicted in Fig. 6. The levers 8.1 and 8.2 were equipped with horizontally relocatable counter-masses ($m_{C1}, m_{C2.1}, m_{C2.2}$). The cylindrical counter-masses were mounted to threaded rods clamped to the monolithic weighing cell structure. Smaller horizontal trim masses realized the fine-adjustment (m_{CF1}, m_{CF2}). The fine adjustment was realized with actuators under high vacuum conditions using a special interface. Despite of imperfections in the adjustment device, the achievable minimal stiffness is fundamentally limited by two temperature-induced effects:

- The temperature coefficient of the YOUNGs modulus of aluminum alloy is in the range of $1{\cdot}10^{-4}\,\mathrm{K}^{-1}$. Assuming a temperature fluctuation during and after the adjustment of the weighing cell mechanism of $0.1\,\mathrm{K}$, the stiffness variation amounts to $\approx 5.5{\cdot}10^{-4}\,\mathrm{N\,m}^{-1}$, which fundamentally limits the achievable minimal absolute value of the stiffness.
- The in-situ measurement of the stiffness involving the EMFC components is another temperature induced variation source. Here, the relative temperature coefficient of the permanent magnet is dominant, which is in the range of $0.4{\cdot}10^{-3}\,\mathrm{K}^{-1}$. Temperature compensation measures are capable of further reducing the temperature effect.

The monolithic weighing cell of the advanced stiffness compensation prototype (PROT-ASC) prototype is presented in the photograph in Figure 12a. The first tests after the assembly of the weighing cell were proof-of-concept measurements with a constant load of $1\,\mathrm{kg}$ and manual adjustments. These measurements aim at a verification of the stiffness adjustment concept and the developed mechanical models. The measurements were conducted under atmospheric conditions.

The effect of a contrary horizontal displacement of the counter masses within the finite element (FE) is shown in Figure 7. The gradient predicted by the analytic rigid-body model (3) is slightly larger. The difference in gradient between FE model and measurement may result from the preliminary nature of the measurements or from effects which are not covered by the FE model.
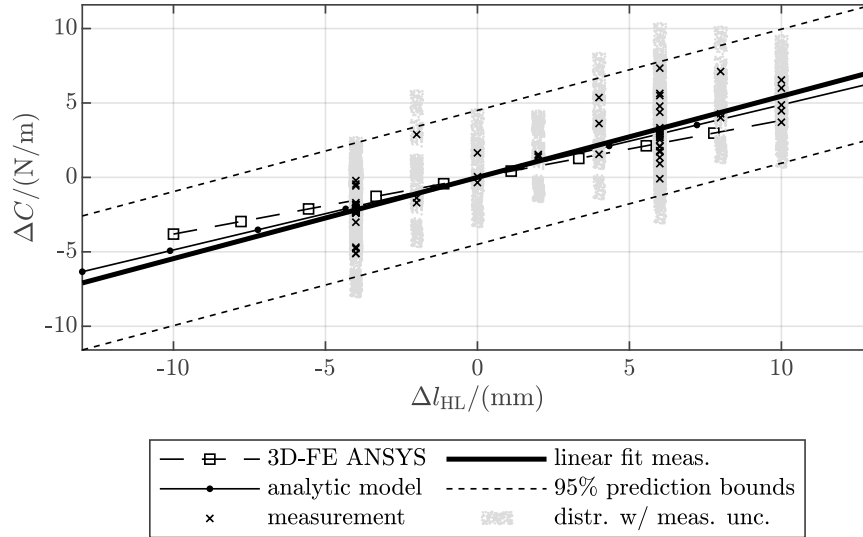

Figure 7: Modeling the stiffness coarse adjustment based on the two nested levers of the PROT-ASC weighing cell shown in Fig. 3. The counter masses have a mass of $m_C = 2 \cdot 170\,\text{g}$ and the geometric parameters are $h_{H1G1} = 9.715\,\text{mm}$ and $h_{H2G2} = -0.285\,\text{mm}$.

3.2. TWO AXIS TILT SENSITIVITY

The novel weighing cell structure is designed to significantly simplify the adjustment process in terms of tilt sensitivity. Typically, tilt sensitivity refers to pitching motion of the weighing cell relative to the vector of gravitational acceleration. The pitching motion is a rotation about the y axis, see Figure 1. However, during operation rotations about the x and y axis occur with equal probability. The tilt sensitivity for a pitching angular displacement Θ is adjustable using a vertical trim masses on the force transmission system (see m_{T8} and m_{T8F} in Figure 6). The separated measurement lever in the new concept minimizes the tilt sensitivity for a rolling angular displacement Φ by structural decoupling.

3.3. OFF-CENTER LOAD SENSITIVITY

Off-center load sensitivity describes the sensitivity of a weighing cell towards eccentrically placed masses on the weighing pan. An eccentric placement of the sample mass introduces an additional static moment and leads to a measurement error in case the weighing cell is off-center load sensitive. The off-center load sensitivity is especially relevant for top-loaded weighing cell with fixed weighing pans. A gimballed hanging weighing pan significantly reduces the introduced static moment by a factor of 2615 for a pendulum length of $l = 400\,\text{mm}$, a mass of $m_{S5} = 1.2\,\text{kg}$, and a gimbal rotational stiffness of $c_{E,x} = 14.6\,\text{N}\,\text{mm}\,\text{rad}^{-1}$. However, for most demanding measurements, the off-center load sensitivity must be minimized by adjustment.

The adjustment of the parallelogram guide of the weighing cell is checked using a geometrically nonlinear calculation in ANSYS®. A schematic of the model is provided in Figure 8. Here, the effect of an asymmetric adjustment on the off-center load sensitivity E_{Ly} can be observed see Figures 9 and 10.
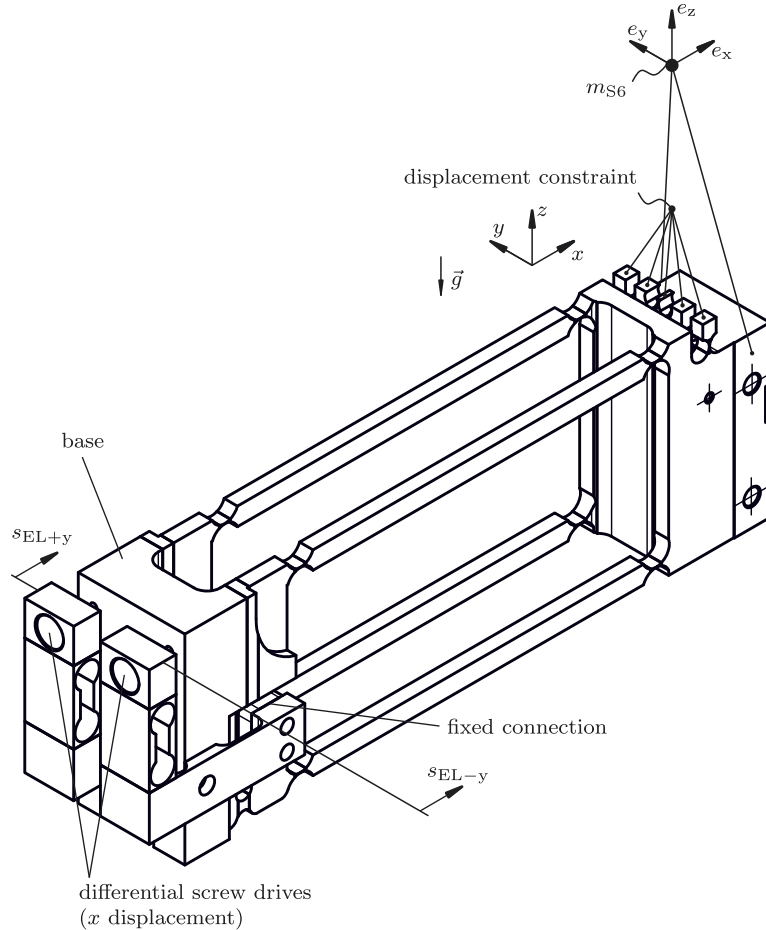

Figure 8: Schematic of the model used to determine the off-center load sensitivity.

Parametric studies in which the force application point for gimbal of hanging weighing pan was shifted showed an effect on the location of the common zero crossing that is shown for nominal conditions in Figure 10. The simulation proves that the off-center load sensitivity in both lateral directions can be adjusted to zero. The achievable values are restricted by the design of the overall adjustment process including the measurement of the off-center load sensitivities.

3.4. IN-VACUO ADJUSTMENT CAPABILITY

The tolerance limits put high demands on measuring the mechanical properties of the EMFC weighing cell. To reliably reach an adjustment state within the tolerances, the weighing cell needs to be placed in a highly stable environment. In-situ adjustment under vacuum conditions is required.

In weighing technology, the air density ρ_a of the air surrounding the weighing device is of high relevance. The buoyancy force, acting on every body of the weighing system, is directly
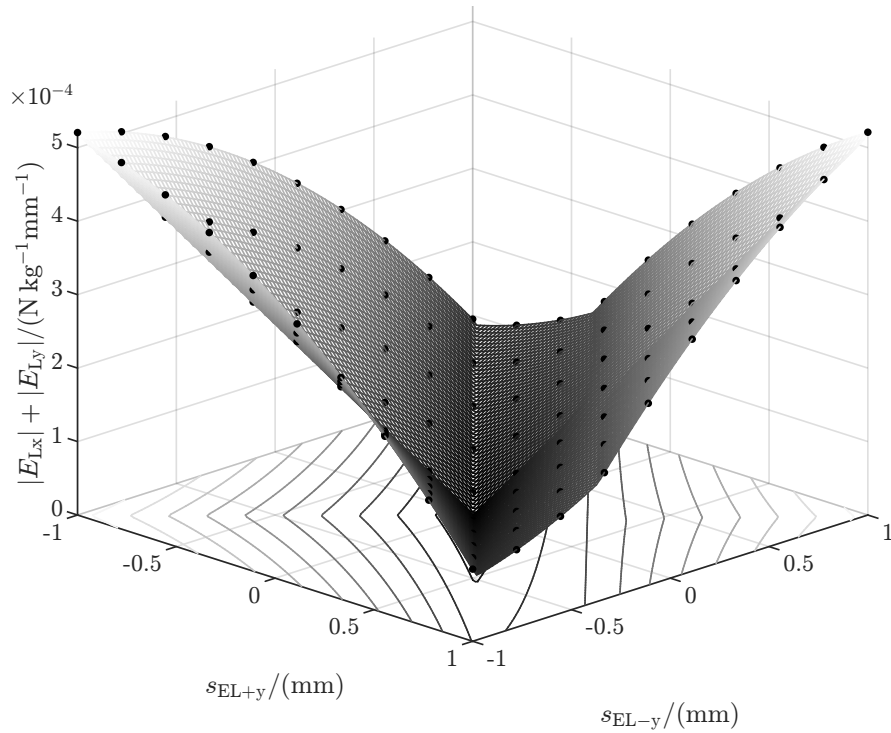
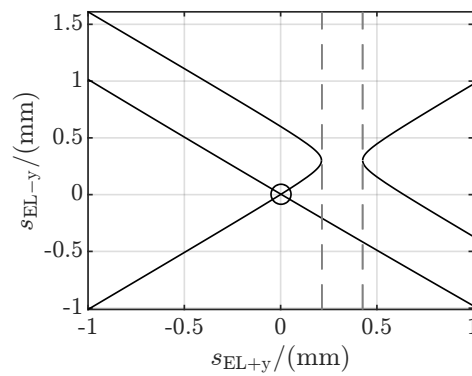Figure 9: Adjustment of the summed absolute values of both lateral off-center load sensitivities.

Figure 10: Common zero crossing for E_{Lx} and E_{Ly} in the adjustment plane indicated by the circle.

proportional to the density. Like a vessel in water, every part of the weighing cell with a specific volume is lifted by a certain buoyancy force in air. The sensitivity to a variation of air pressure on the static equilibrium of a balance in terms of error torque can be calculated as follows:

$$\frac{dM}{d\rho_a} = \rho_a \sum_{i=1}^{N} V_i L_i$$

The design of a weighing cell involving parts with different densities of the materials can be carefully adjusted to a buoyancy insensitive state: A solution of the linear equation system has to be found:

$$0 = g \sum_{i=1}^{N} \rho_i V_i L_i$$

$$0 = g \sum_{i=1}^{N} \rho_a V_i L_i$$

The in-vacuo adjustment requires automation. Four drives were required for the adjustment of C and D_Θ, see Figure 11. The choice concerning the fine adjustment of C and D_Θ fell on vacuum compatible stepper motors. After each adjustment step, the adjustment drives have to be fully mechanically decoupled to measure the adjustment state regarding stiffness and tilt sensitivity. A slot-screw-driver-type coupling with sufficient backlash and with compensation of lateral misalignment was designed. To measure the tilt sensitivity after each adjustment steps in the closed vacuum chamber, the base of the weighing cell needed to be tilted. The tilt angle was introduced by a vacuum-compatible linear drive which was vertically mounted to the weighing cell's base structure at the back of the assembly. After the final adjustment step, the adjustment unit can be fully removed from the vacuum chamber to avoid any disturbance during final operation.

4. CONCLUDING SUMMARY

The novel weighing cell includes numerous features that enable a reduction of all considered mechanical error sources: stiffness, tilt sensitivity, and off-center load sensitivity. A summary is provided in the following list:

- adjustability of all considered mechanical first-order sensitivities: stiffness, tilt sensitivity, and off-center load sensitivity,

- compensation of manufacturing deviations related to the elastic stiffness,

- independent rough and fine adjustment of stiffness and tilt sensitivity,

- adjustability of the bouyancy independence or sensitivity to changes in air pressure,

- adjustability of the tilt sensitivity,

- two-axis adjustability if the off-center load sensitivity,

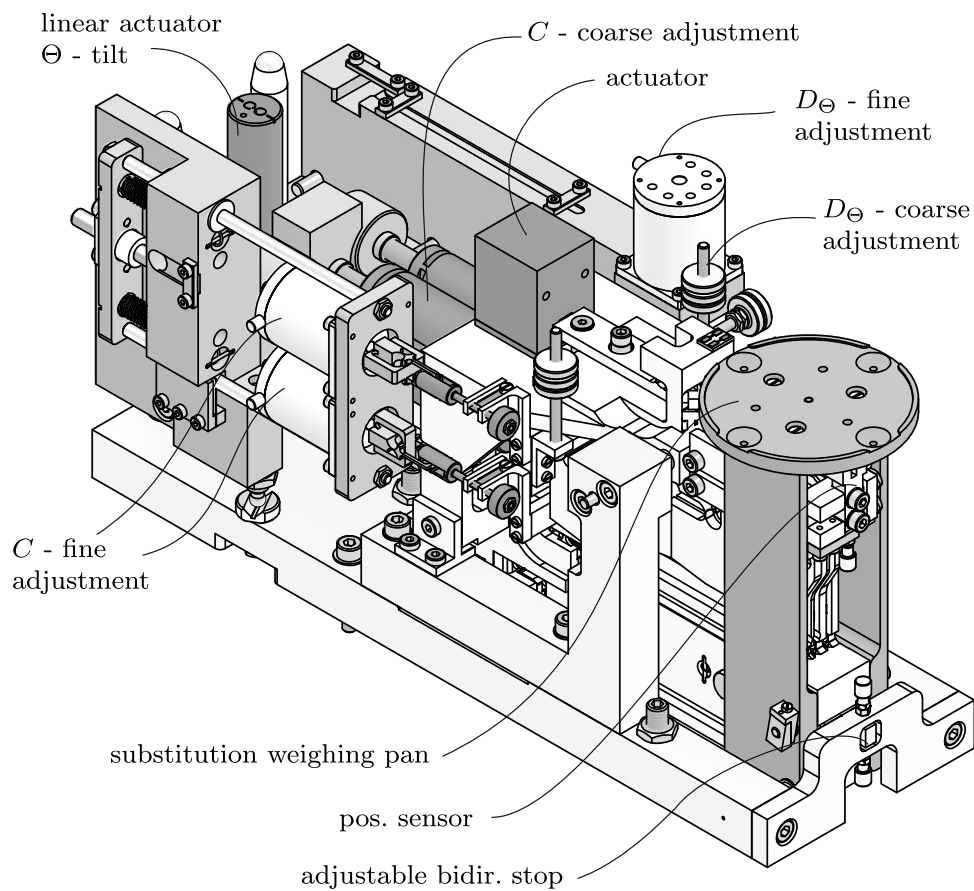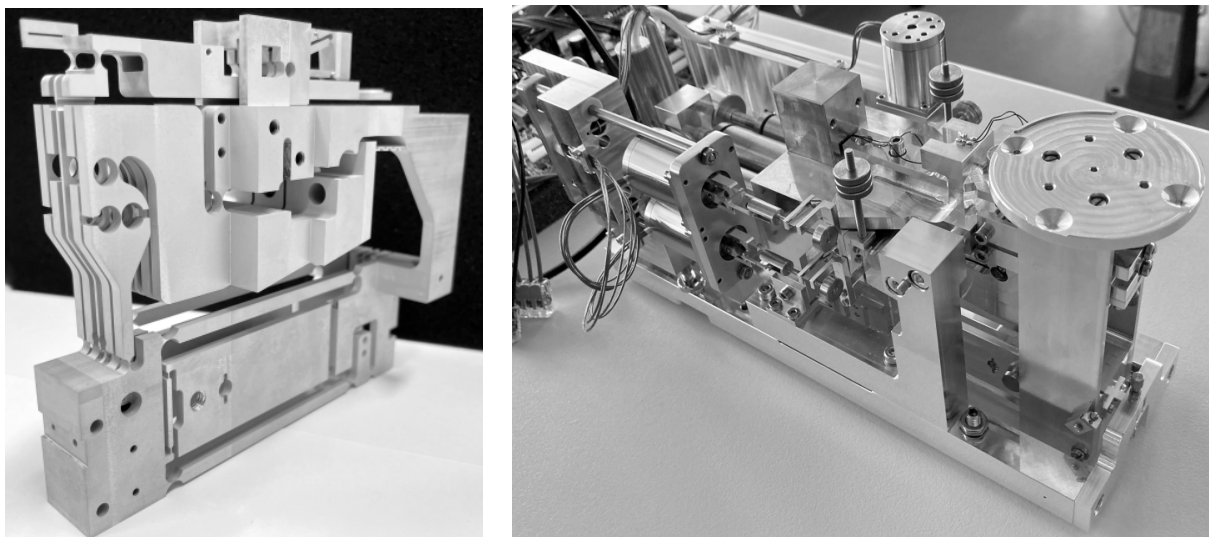- establishing a force and metrology loop within a mass comparator,

Figure 11: Complete EMFC weighing cell subsystem of the vacuum mass comparator with adjustment unit for stiffness and tilt sensitivity.

(a) Novel weighing cell mechanism with manufacturing fixtures.

(b) Complete system of the weighing cell system with adjustment devices.

Figure 12: Manufactured weighing cell and complete assembly including the in-vacuo adjustment unit.

- largely monolithic design, except for weighing pan, adjustment devices, and EMFC components.

The developed EMFC weighing cell mechanism approaches the mechanically ideal mass comparator in the considered aspects: stiffness, tilt sensitivity and off-center load sensitivity. It was ensured that these properties are adjustable to within their respective tolerance limit in order to achieve 5 ng uncertainty in a single weighing. Furthermore, the concept and design particularities minimized the cross-sensitivities between the parameters. Except for the rough adjustment of the stiffness, all other adjustment have not yet been experimentally verified. However, their effectivity was proven by numerical simulation. The experimental test of all adjustment measures and later the proof of the in-vacuo adjustability are the next steps.

REFERENCES

[1] M. Darnieder et al. Static behavior of weighing cells. *Journal of Sensors and Sensor Systems* 7.2 (2018), pp. 587–600.

[2] S. T. Smith and D. G. Chetwynd. *Foundations of ultraprecision mechanism design*. Vol. v. 2. Developments in nanotechnology. Yverdon, Switzerland: Gordon and Breach Science Publishers, 1992.

ACKNOWLEDGEMENT

CONTACTS
M.Sc. Maximilian Darnieder   max.darnieder@outlook.de